γp and $\gamma\gamma$ scattering from $\bar{p}p$, pp forward amplitudes in a QCD eikonal model with a dynamical gluon mass

E. G. S. Luna[1,2] and A. A. Natale[1]

[1]*Instituto de Física Teórica, UNESP, São Paulo State University, 01405-900, São Paulo, SP, Brazil*
[2]*Instituto de Física Gleb Wataghin, Universidade Estadual de Campinas, 13083-970, Campinas, SP, Brazil*
(Received 20 February 2006; published 26 April 2006)

We examine the γp photoproduction and the hadronic $\gamma\gamma$ total cross sections by means of a QCD eikonal model with a dynamical infrared mass scale. In this model, where the dynamical gluon mass is the natural regulator for the tree level gluon-gluon scattering, the γp and $\gamma\gamma$ total cross sections are derived from the pp and $\bar{p}p$ forward scattering amplitudes assuming vector meson dominance and the additive quark model. We show that the validity of the cross section factorization relation $\sigma_{pp}/\sigma_{\gamma p} = \sigma_{\gamma p}/\sigma_{\gamma\gamma}$ is fulfilled depending on the Monte Carlo model used to unfold the hadronic $\gamma\gamma$ cross section data, and we discuss in detail the case of $\sigma(\gamma\gamma \to \text{hadrons})$ data with $W_{\gamma\gamma} > 10$ GeV unfolded by the Monte Carlo generators PYTHIA and PHOJET. The data seems to favor a mild dependence with the energy of the probability (P_{had}) that the photon interacts as a hadron.

DOI: 10.1103/PhysRevD.73.074019 PACS numbers: 12.38.Lg, 13.85.Dz, 13.85.Lg

I. INTRODUCTION

The hadronic nature of the photon is currently a subject of intense theoretical and experimental interest. The central question for hadronic interactions of real photons is whether they behave the same as hadrons or whether the additional hard contributions to the total cross sections of photon-induced interactions lead to a faster rise of the total $\gamma\gamma$ and γp cross sections as a function of the energy.

The increase of hadron-hadron total cross sections was theoretically predicted many years ago [1] and this prediction has been accurately verified by experiment [2]. The measurements of the total photoproduction cross sections $\sigma^{\gamma p}$ at HERA [3,4] and the measurements of the total hadronic cross sections $\sigma^{\gamma\gamma}$ at LEP [5,6] have also established the increase of photon-hadron and photon-photon total cross sections. Early modeling of these cross sections within Regge theory shows a energy dependence similar to the ones of nucleon-nucleon [7]. This universal behavior, appropriately scaled in order to take into account the differences between hadrons and the photon, can be understood as follows: at high center-of-mass energies the total photoproduction $\sigma^{\gamma p}$ and the total hadronic cross section $\sigma^{\gamma\gamma}$ for the production of hadrons in the interaction of one and two real photons, respectively, are expected to be dominated by interactions where the photon has fluctuated into a hadronic state. Therefore measuring the energy dependence of photon-induced processes should improve our understanding of the hadronic nature of the photon as well as the universal high-energy behavior of total hadronic cross sections.

However the comparison of the experimental data and the theoretical prediction, as discussed some time ago [8], may also present some subtleties depending on the Monte Carlo model used to analyze the data. Despite the similar energy dependence of hadron-hadron, photon-hadron and photon-photon total cross sections, there are significant differences between photon-induced cross section measurements and those of the purely hadronic processes. The latter comes from a counting rate $\Delta N(t)$, the number of counts/ $\sec/\Delta t$ in a narrow interval around the four-momentum transfer squared t, extrapolated to the value $\Delta N(t = 0)$ and normalized by an appropriate factor (for colliding beams this normalization factor is the luminosity L). The $\gamma\gamma$ cross sections are extracted from a measurement of hadron production in e^+e^- processes and are strongly dependent upon the acceptance corrections to be employed. These corrections are in turn sensitive to the Monte Carlo models used in the simulation of the different components of an event, and this general procedure produces uncertainties in the determination of $\sigma^{\gamma\gamma}$ [8]. This clearly implies that any phenomenological analysis has to take properly into account the discrepancies among $\sigma^{\gamma\gamma}$ data obtained from different Monte Carlo generators.

A global description of photon-photon, photon-hadron and hadron-hadron total cross sections is possible by means of QCD-inspired eikonal models [9–12]. In these models the increase of the total cross sections is associated with semihard scatterings of partons in the hadrons. The energy dependence of the cross sections is driven mainly by gluon-gluon scattering processes, since $g(x, Q^2) \gg q(x, Q^2)$ at small-x values. Nevertheless, the gluon-gluon subprocess cross section is potentially divergent at small transferred momenta, and the usual procedure to regulate this behavior is the introduction of a purely *ad hoc* parameter separating the perturbative from the nonperturbative QCD region, like an infrared mass scale [9,13,14], or a cut-off at low transverse momentum p_T [10–12,15]. These arbitrary parameters are adjusted in order to obtain the best fits to the experimental data.

Recently we introduced a QCD-inspired eikonal model where the *ad hoc* infrared mass scale was substituted by a

dynamical gluon mass one [16]. One of the central advantages of the model is that it gives a precise physical meaning for the quoted infrared scale. Furthermore, since the behavior of the running coupling constant is constrained by the value of dynamical gluon mass [17], the model also has a smaller number of parameters than similar models.

In this work we perform a detailed study of the γp and $\gamma\gamma$ scattering in the framework of the QCD eikonal model with a gluon dynamical mass of Ref. [16]. We address the question of derivating γp and $\gamma\gamma$ total cross sections from the pp and $\bar{p}p$ forward amplitudes, exploring the process underlying the extraction of $\gamma\gamma$ from the e^+e^- data. The paper is organized as follows: in the next section we briefly review the QCD-inspired eikonal model with a dynamical gluon mass. Sec. III contains the details of $\gamma\gamma$ and γp cross sections calculations. The results are presented in the Sec. IV, where we provide fits for the cross sections, discuss the factorization theorem, $\sigma_{pp}/\sigma_{\gamma p} = \sigma_{\gamma p}/\sigma_{\gamma\gamma}$, and investigate a possible mild dependence of the probability that the photon interacts as a hadron ($P_{\rm had}$) increases with the energy. The results are compared to the data handled with the PYTHIA and PHOJET Monte Carlo generators. The conclusions are drawn in Sec. V.

II. A QCD-INSPIRED EIKONAL MODEL WITH A DYNAMICAL SCALE

The high-energy hadron-hadron cross sections are calculated using a recently developed QCD-inspired eikonal model, where the onset of the dominance of gluons in the interaction of high-energy hadrons is managed by the dynamical gluon mass scale [16]. The model satisfies analyticity and unitarity constraints, and the hadron-hadron elastic scattering is due to the diffractive shadow of inelastic events. In the eikonal formalism the total cross section is given by

$$\sigma_{\rm tot}(s) = 4\pi \int_0^\infty bdb[1 - e^{-\chi_I(b,s)}\cos\chi_R(b,s)], \quad (1)$$

where s is the square of the total center-of-mass energy, b is the impact parameter, and $\chi(b,s) = \chi_R(b,s) + i\chi_I(b,s)$ is a complex eikonal function. Following the Ref. [16], we write the even eikonal as the sum of gluon-gluon, quark-gluon, and quark-quark contributions:

$$\begin{aligned}\chi^+(b,s) &= \chi_{qq}(b,s) + \chi_{qg}(b,s) + \chi_{gg}(b,s)\\ &= i[\sigma_{qq}(s)W(b;\mu_{qq}) + \sigma_{qg}(s)W(b;\mu_{qg})\\ &\quad + \sigma_{gg}(s)W(b;\mu_{gg})], \end{aligned} \quad (2)$$

where $\chi^{\bar{p}p}_{pp}(b,s) = \chi^+(b,s) \pm \chi^-(b,s)$. Here $W(b;\mu)$ is the overlap function at impact parameter space and $\sigma_{ij}(s)$ are the elementary subprocess cross sections of colliding quarks and gluons ($i, j = q, g$). The overlap function, normalized so that $\int d^2\vec{b}W(b;\mu) = 1$, is associated with the Fourier transform of a dipole form factor,

$$W(b;\mu) = \frac{\mu^2}{96\pi}(\mu b)^3 K_3(\mu b), \quad (3)$$

where $K_3(x)$ is the modified Bessel function of second kind. The odd eikonal $\chi^-(b,s)$, that accounts for the difference between pp and $\bar{p}p$ channels, is parametrized as

$$\chi^-(b,s) = C^-\Sigma\frac{m_g}{\sqrt{s}}e^{i\pi/4}W(b;\mu^-), \quad (4)$$

where m_g is the dynamical gluon mass and the parameters C^- and μ^- are constants to be fitted. The factor Σ is defined as

$$\Sigma = \frac{9\pi\bar{\alpha}_s^2(0)}{m_g^2}, \quad (5)$$

with the dynamical coupling constant $\bar{\alpha}_s$ set at its frozen infrared value. The origin of the dynamical gluon mass and the frozen coupling constant can be traced back to the early work of Cornwall [18], and the formal expressions of these quantities can be seen in Ref. [16].

Since that the main contribution to the asymptotic behavior of hadron-hadron total cross sections comes from gluon-gluon semihard collisions, the eikonal functions $\chi_{qq}(b,s)$ and $\chi_{qg}(b,s)$, needed to describe the lower-energy forward data, are simply parametrized with terms dictated by the Regge phenomenology:

$$\chi_{qq}(b,s) = i\Sigma A\frac{m_g}{\sqrt{s}}W(b;\mu_{qq}), \quad (6)$$

$$\chi_{qg}(b,s) = i\Sigma\left[A' + B'\ln\left(\frac{s}{m_g^2}\right)\right]W(b;\sqrt{\mu_{qq}\mu_{gg}}), \quad (7)$$

where A, A', B', μ_{qq} and μ_{gg} are fitting parameters.

In the model the gluon eikonal term $\chi_{gg}(b,s)$ (see the expression (2)) is written as $\chi_{gg}(b,s) \equiv \sigma_{gg}^{\rm DPT}(s)W(b;\mu_{gg})$, where

$$\sigma_{gg}^{\rm DPT}(s) = C'\int_{4m_g^2/s}^1 d\tau F_{gg}(\tau)\hat{\sigma}_{gg}^{\rm DPT}(\hat{s}). \quad (8)$$

Here $F_{gg}(\tau)$ is the convoluted structure function for pair gg, $\hat{\sigma}_{gg}^{\rm DPT}(\hat{s})$ is the subprocess cross section and C' is a fitting parameter. In the above expression it is introduced the energy threshold $\hat{s} \geq 4m_g^2$ for the final state gluons, assuming that these are screened gluons [19]. The structure function $F_{gg}(\tau)$ is given by

$$F_{gg}(\tau) = [g \otimes g](\tau) = \int_\tau^1 \frac{dx}{x}g(x)g\left(\frac{\tau}{x}\right), \quad (9)$$

where $g(x)$ is the gluon distribution function, adopted as [9]

$$g(x) = N_g\frac{(1-x)^5}{x^J}, \quad (10)$$

where $J = 1 + \epsilon$ and $N_g = \frac{1}{240}(6-\epsilon)(5-\epsilon)\ldots(1-\epsilon)$. The correct analyticity properties of the model amplitudes is ensured by substituting $s \rightarrow se^{-i\pi/2}$ throughout Eqs. (6)–(8). Other details of the model can be seen in

TABLE I. Values of the parameters of the DGM model resulting from the global fit to the forward pp and $\bar{p}p$ data [16]. The dynamical gluon mass scale was set to $m_g = 400$ MeV.

C'	$(12.097 \pm 0.962) \times 10^{-3}$
μ_{gg} [GeV]	0.7242 ± 0.0172
A	6.72 ± 0.92
μ_{qq} [GeV]	1.0745 ± 0.0405
A'	$(4.491 \pm 0.179) \times 10^{-3}$
B'	1.08 ± 0.14
C^-	3.17 ± 0.35
μ^- [GeV]	0.6092 ± 0.0884

Ref. [16], and the fitting parameters are shown in Table I, in the case of a dynamical gluon mass $m_g = 400$ MeV, which is the preferred value for pp and $\bar{p}p$ scattering.

III. PHOTON-PROTON AND PHOTON-PHOTON REACTIONS

The total cross section $\sigma_{\rm tot}$, the ratio of the real to the imaginary part of the forward scattering amplitude ρ, and the nuclear slope B for proton-proton and antiproton-proton collisions have been found to be well described by the QCD-inspired eikonal model discussed in the last section, which we shall refer simply as the DGM model. Hence we fix the input parameters to the eikonal model calculations by using the data on pp and $\bar{p}p$ reactions in order to make predictions for $\sigma^{\gamma p}$ and $\sigma^{\gamma\gamma}$ using the same values of the parameters. These values are shown in the Table I.

The fact that at high energies a photon can fluctuate itself into a hadronic state open many theoretical possibilities. For example, in the model of Block *et al.* [9] the data on γp total photoproduction and the total hadronic $\gamma\gamma$ cross sections can be derived from the pp and $\bar{p}p$ forward amplitudes using vector meson dominance (VMD) and the additive quark model. We verify that this procedure, valid for QCD-inspired models with an arbitrary infrared scale, can also be applied to our eikonal model with a dynamical gluon mass being necessary only minimal changes displayed in the sequence. Thus, considering that a strongly interacting photon behaves as a system of two quarks (the additive quark model), the even amplitude for γp scattering can be obtained after the substitutions $\sigma_{ij} \to \frac{2}{3}\sigma_{ij}$ and $\mu_{ij} \to \sqrt{\frac{3}{2}}\mu_{ij}$ in the eikonal of Eq. (2), resulting in the following expression:

$$\chi^+_{\gamma p}(b,s) = i\frac{2}{3}\Big[\sigma_{qq}(s)W\Big(b;\sqrt{\frac{3}{2}}\mu_{qq}\Big) + \sigma_{qg}(s)W\Big(b;\sqrt{\frac{3}{2}}\mu_{qg}\Big) + \sigma_{gg}(s)W\Big(b;\sqrt{\frac{3}{2}}\mu_{gg}\Big)\Big]. \quad (11)$$

Note that in the work of Block *et al.* [9] the above procedure is used to obtain directly the physical eikonal $\chi^{\gamma p}(b,s)$, what means that the odd part of the eikonal that describes pp and $\bar{p}p$ scattering is neglected, and $\chi^{\gamma p}(b,s) \equiv \chi^+_{\gamma p}(b,s)$. This is a good approximation at high energies, where the total cross sections pp and $\bar{p}p$ are asymptotically expected to be the same. However, below $\sqrt{s} \sim 100$ GeV the pp and $\bar{p}p$ total cross sections are different, as happens in other channels like $\pi^- p$ and $\pi^+ p$ as well as $K^- p$ and $K^+ p$. Therefore it is reasonable to expect the same behavior for the channels γp and $\gamma\bar{p}$. To account for these possible differences at low energy in the case of $\sigma^{\gamma p}$ and $\sigma^{\gamma\bar{p}}$ we apply the prescription dictated by the additive quark model also in the odd eikonal of Eq. (4),

$$\chi^-_{\gamma p}(b,s) = \frac{2}{3}C^-\Sigma\frac{m_g}{\sqrt{s}}e^{i\pi/4}W\Big(b;\sqrt{\frac{3}{2}}\mu^-\Big), \quad (12)$$

and the full physical eikonal, combining the even and odd parts, will be finally given by $\chi^{\gamma\bar{p}}_{\gamma p} = \chi^+_{\gamma p}(b,s) \pm \chi^-_{\gamma p}(b,s)$.

Assuming vector meson dominance (VMD), the eikonalized γp total cross section can be written as

$$\sigma^{\gamma p}_{\rm tot}(s) = 4\pi P^{\gamma p}_{\rm had}\int_0^\infty bdb\rho\rho[1 - e^{-\chi^{\gamma p}_I(b,s)}\cos\chi^{\gamma p}_R(b,s)], \quad (13)$$

where $P^{\gamma p}_{\rm had}$ is the probability that the photon interacts as a hadron. In the simplest VMD formulation this probability is expected to be of $\mathcal{O}(\alpha_{\rm em})$:

$$P^{\gamma p}_{\rm had} = P_{\rm had} = \sum_{V=\rho,\omega,\phi}\frac{4\pi\alpha_{\rm em}}{f_V^2} \sim \frac{1}{249}, \quad (14)$$

where ρ, ω and ϕ are vector mesons. However, there are expected contributions to $P_{\rm had}$ other than ρ, ω, ϕ. For example, in the eikonalized minijet model analysis of $\sigma^{\gamma\gamma}$ of the Ref. [11] a good fit to the photoproduction data is obtained with the value $P_{\rm had} = 1/204$, which includes a non-VMD contribution of $\mathcal{O}(20\%)$. In this case there are strong contributions of heavier vector mesons and continuum states. Moreover, the probability $P_{\rm had}$ may also depend on the energy, which is a possibility that we will explore in this paper.

To extend the model to the $\gamma\gamma$ channel we just perform the substitutions $\sigma_{ij} \to \frac{4}{9}\sigma_{ij}$ and $\mu_{ij} \to \frac{3}{2}\mu_{ij}$ in the even part of the eikonal (Eq. (2)):

$$\chi^{\gamma\gamma}(b,s) = i\frac{4}{9}\Big[\sigma_{qq}(s)W\Big(b;\frac{3}{2}\mu_{qq}\Big) + \sigma_{qg}(s)W\Big(b;\frac{3}{2}\mu_{qg}\Big) + \sigma_{gg}(s)W\Big(b;\frac{3}{2}\mu_{gg}\Big)\Big]; \quad (15)$$

hence the additive quark model and the VMD are again assumed to be valid, and the calculation leads to the following eikonalized total $\gamma\gamma$ hadronic cross section

$$\sigma_{\rm tot}^{\gamma\gamma}(s) = 4\pi P_{\rm had}^{\gamma\gamma} \int_0^\infty bdb[1 - e^{-\chi_I^{\gamma\gamma}(b,s)} \cos\chi_R^{\gamma\gamma}(b,s)] \tag{16}$$

where

$$P_{\rm had}^{\gamma\gamma} = P_{\rm had}^2. \tag{17}$$

With the eikonal parameters of the DGM model fixed by the pp and $\bar{p}p$ data (Table I), we have performed all calculations of photoproduction and photon-photon scattering. Apart from the equations that we have displayed above, we will introduce two possible modifications when we present our results in the next section. One is related to a feasible energy dependence of $P_{\rm had}$, and the other is concerned with the requirement of a normalization factor in the $\sigma^{\gamma\gamma}$ calculation.

IV. RESULTS

In our analysis the center-of-mass energy thresholds for the γp and $\gamma\gamma$ channels are the same that one used in the study of the pp and $\bar{p}p$ channels: $\sqrt{s}_{\gamma p}^{\rm min} = W_{\gamma\gamma}^{\rm min} =$ 10 GeV. We adopt a χ^2 fitting procedure, assuming an interval $\chi^2 - \chi^2_{\rm min}$ corresponding, in the case of normal errors, to the projection of the χ^2 hypersurface containing 90% of probability. In the case of 1, 2 and 3 free parameters, this corresponds to the interval $\chi^2 - \chi^2_{\rm min} = 2.70$, 4.61 and 6.25, respectively. We use the data set for $\sigma^{\gamma p}$ compiled and analyzed by the Particle Data Group (PDG) [2], with the statistic and systematic errors added in quadrature. Data on $\gamma\gamma$ total hadronic cross sections are also available on the PDG compilation, but the $\gamma\gamma$ data quoted by the PDG are the average of the results obtained by unfolding the data with the PYTHIA [20] and the PHOJET [21] Monte Carlo generators. These event generators, based on a model by Schuler and Sjöstrand [22] (PYTHIA) and on the Dual Parton model [23] (PHOJET), are used to simulate photon-photon interactions and, in general, data unfolded with PYTHIA are higher than if unfolded with PHOJET. As a consequence we obtain totally different scenarios for the rise of the total hadronic $\gamma\gamma$ cross section at high energies. For this reason, we have deconvoluted the data on $\sigma^{\gamma\gamma}$ of the L3 [5] and OPAL [6] collaborations, according to whether PYTHIA or PHOJET was used. Therefore, instead of using the PDG data for $\sigma^{\gamma\gamma}$, we performed global fits considering separately the data obtained through the PYTHIA and PHOJET codes, defining two data sets as

SET I: $\sigma^{\gamma p}$ and $\sigma_{\rm PYT}^{\gamma\gamma}$ data ($\sqrt{s}_{\gamma p}, W_{\gamma\gamma} \geq 10$ GeV),

SET II: $\sigma^{\gamma p}$ and $\sigma_{\rm PHO}^{\gamma\gamma}$ data ($\sqrt{s}_{\gamma p}, W_{\gamma\gamma} \geq 10$ GeV),

where $\sigma_{\rm PYT}^{\gamma\gamma}$ ($\sigma_{\rm PHO}^{\gamma\gamma}$) correspond to the data of $\gamma\gamma$ total hadronic cross section obtained via the PYTHIA (PHOJET) generator. The unfolded results are depicted in the Fig. 1. This strategy of analysis is similar to the one adopted by Block and Kang, where a global test of factorization for nucleon-nucleon, γp and $\gamma\gamma$ scattering was performed through real analytic amplitudes [24]. Their results have evidenced the critical role played by the Monte Carlo simulations used by L3 and OPAL group.

Our first analysis (henceforth referred to as FIT I) consisted in the determination of the $P_{\rm had}^{-1}$ values from fits to the data sets defined above. In the fit to the SET I we obtained $P_{\rm had}^{-1} = 220.85 \pm 0.59$; the χ^2/DOF for this fit was 3.29. The fit to the SET II has resulted in $P_{\rm had}^{-1} = 223.70 \pm 0.50$, with $\chi^2/{\rm DOF} = 1.94$. These values are shown in Table II. The $\sigma^{\gamma p}$ and $\sigma^{\gamma\gamma}$ cross sections corresponding to these values of $P_{\rm had}^{-1}$ are shown by the solid curves in Fig. 2. The results of the fit to the SET I are displayed in Figs. 2(a) and 2(b), whereas the results of the fit to the SET II are displayed in Figs. 2(c) and 2(d). In the FIT I the χ^2/DOF values are relatively high. However, as we already commented, the extraction of $\gamma\gamma$ data from e^+e^- processes is strongly sensitive to the Monte Carlo simulation, and this procedure could require a systematic overall-normalization factor in the experimental data. In fact, the cross section $\sigma(\gamma\gamma \rightarrow) hadrons$ is determined from the differential cross section of the reaction $e^+e^- \rightarrow e^+e^-\gamma^*\gamma^* \rightarrow e^+e^- hadrons$ by means of both the luminosity function $L_{\gamma\gamma}$ for the photon flux and the hadronic cross section $\sigma_{\gamma\gamma}(W_{\gamma\gamma}, Q_1^2, Q_2^2)$ [5,6,25–27]. However, the uncertainty in the cross section extrapolation to real pho-

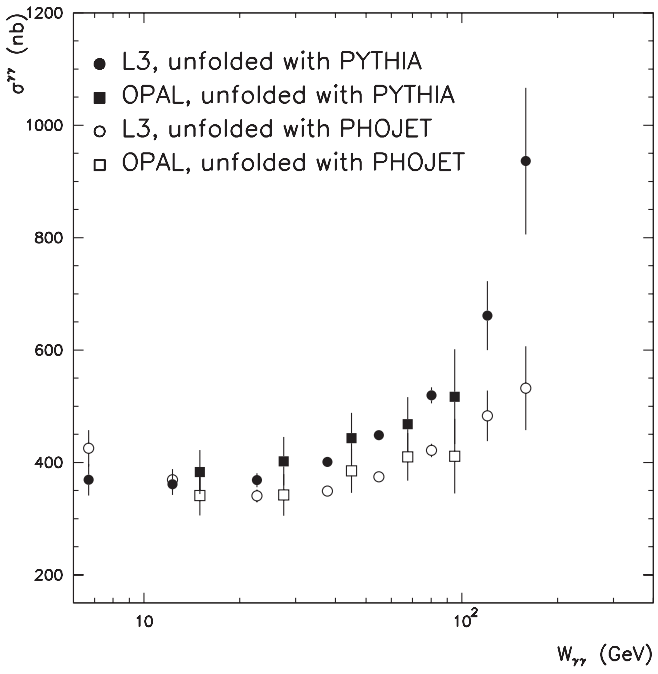

FIG. 1. $\sigma^{\gamma\gamma}$ data from the L3 and OPAL collaborations unfolded with the PYTHIA and PHOJET generators.

TABLE II. Fits adopting $P_{\rm had}$ constant.

	FIT I		FIT II	
	SET I	SET II	SET I	SET II
$P_{\rm had}^{-1}$	220.85 ± 0.59	223.70 ± 0.50	222.30 ± 1.18	222.30 ± 1.71
N	-	-	1.086 ± 0.028	0.936 ± 0.025
χ^2/DOF	3.29	1.94	2.05	1.02
FIGURES	2(a) and 2(b)	2(c) and 2(d)	2(a) and 2(b)	2(c) and 2(d)

tons ($Q_1^2 = Q_2^2 = 0$) is estimated to be 5–7.5%, and this uncertainty is not included in the systematic error of the measurement [27]. In this case we can introduce a normalization factor in the $\sigma^{\gamma\gamma}$ data as performed in Ref. [24] or, what we have chosen to do, just multiply Eq. (16) by a normalization factor N to be fitted by the experiment:

$$\sigma_{\rm tot}^{\gamma\gamma}(s) = 4\pi N P_{\rm had}^{\gamma\gamma} \int_0^\infty bdb[1 - e^{-\chi_I^{\gamma\gamma}(b,s)} \cos\chi_R^{\gamma\gamma}(b, s)]. \tag{18}$$

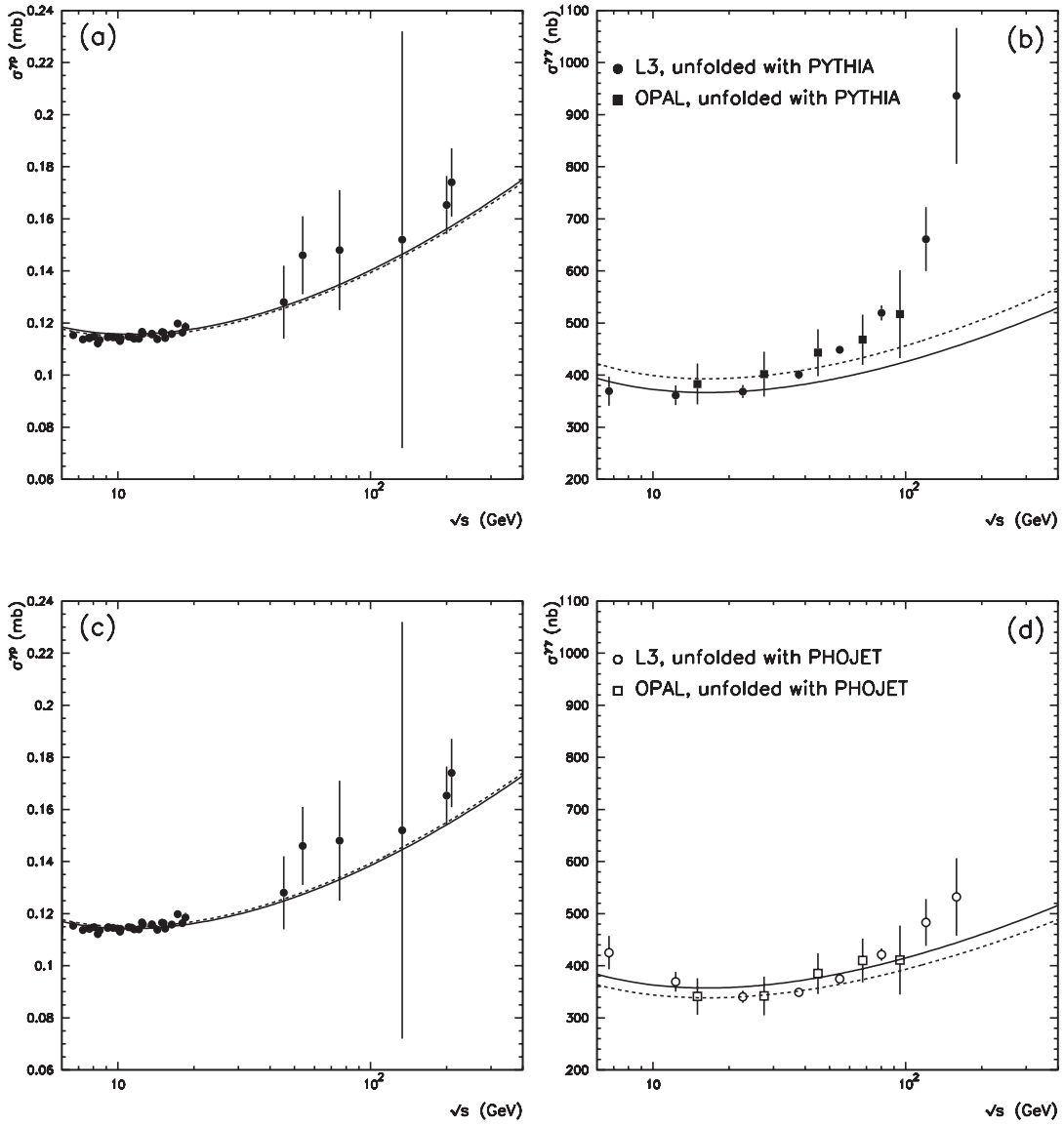

FIG. 2. $\sigma^{\gamma p}$ and $\sigma^{\gamma\gamma}$ cross sections corresponding to the constant values of $P_{\rm had}^{-1}$ shown in Table II. The solid (dashed) curves correspond to the FIT I (II), whereas the results of the fit to the SET I are displayed in Figs. 2(a) and 2(b), and the results of the fit to the SET II are displayed in Figs. 2(c) and 2(d).

TABLE III. Fits adopting $P_{\rm had} = a + b\ln(s)$.

	SET I	SET II
a	$(3.882 \pm 0.122) \times 10^{-3}$	$(4.175 \pm 0.247) \times 10^{-3}$
b	$(1.195 \pm 0.229) \times 10^{-4}$	$(6.272 \pm 4.775) \times 10^{-5}$
N	0.963 ± 0.037	0.875 ± 0.052
χ^2/DOF	0.86	0.76
FIGURES	3(a) and 3(b)	3(c) and 3(d)

Within this approach (henceforth referred to as FIT II) we carried out new fits to the SETS I and II described above. We obtained for the SET I (SET II) the values $P_{\rm had}^{-1} = 222.30 \pm 1.18$ ($P_{\rm had}^{-1} = 220.30 \pm 1.71$) and $N = 1.086 \pm 0.028$ ($N = 0.936 \pm 0.025$), with $\chi^2/\mathrm{DOF} = 2.05$ ($\chi^2/\mathrm{DOF} = 1.02$). These values are shown in Table II. The γp and $\gamma\gamma$ total cross sections corresponding to these values of $P_{\rm had}^{-1}$ and N are shown by the dashed curves in Fig. 2. The results of the fit to the SET I are displayed in Figs. 2(a) and 2(b), whereas the results of the fit to the SET II are displayed in Figs. 2(c) and 2(d). We notice that the approach adopted in the FIT II leads to an improvement of the fits, since the χ^2/DOF values obtained through the FIT II are smaller than ones obtained through the FIT I. These results indicate the convenience of introducing a normalization factor in order to account for possible effects not included in the systematic error of $\sigma^{\gamma\gamma}$ data.

In the sequence we have also explored the possibility that $P_{\rm had}$ varies with the energy. Such possibility has been

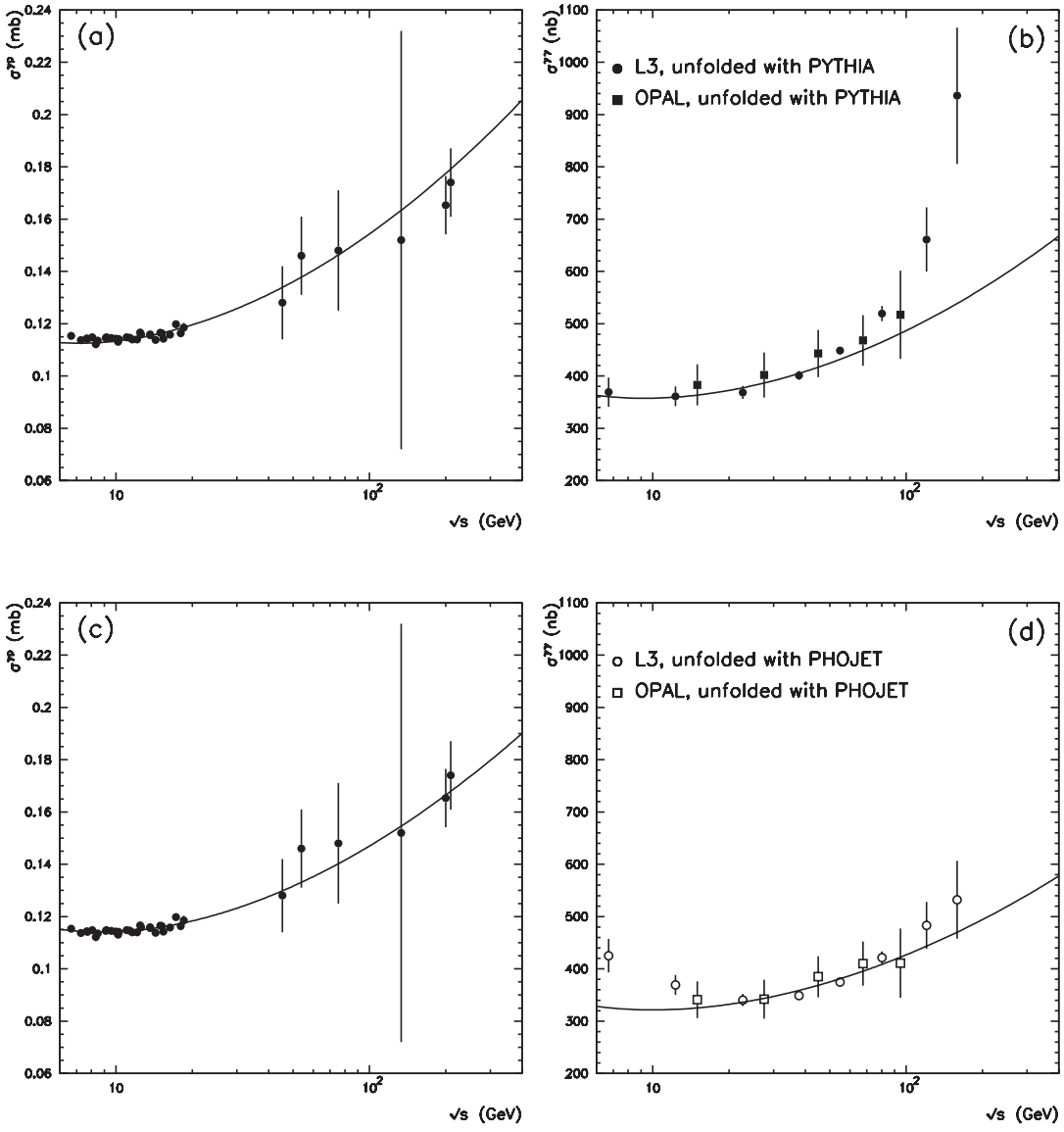

FIG. 3. $\sigma^{\gamma p}$ and $\sigma^{\gamma\gamma}$ cross sections corresponding to the case where $P_{\rm had}^{-1}$ varies with the energy as described in Table III. The curves of Figs. 3(a) and 3(b) are related to the fit labeled as SET I in Table III, whereas the Figs. 3(c) and 3(d) are related to the values of the SET II displayed in the same table.

raised in the past [28], although there are arguments against it [29]. We have assumed a phenomenological expression for $P_{\rm had}$, implying that it increases logarithmically with the square of the center-of-mass energy: $P_{\rm had} = a + b\ln(s)$. Our intention was just to see if the quality of the fit improves in such situation, referred to as FIT III. The results of the fit to the SET I were: $a = (3.882 \pm 0.122) \times 10^{-3}$, $b = (1.195 \pm 0.229) \times 10^{-4}$ and $N = 0.963 \pm 0.037$, with $\chi^2/\mathrm{DOF} = 0.86$. The fit results to the SET II were: $a = (4.175 \pm 0.247) \times 10^{-3}$, $b = (6.272 \pm 4.775) \times 10^{-5}$ and $N = 0.875 \pm 0.052$, with $\chi^2/\mathrm{DOF} = 0.76$. All these results are shown in Table III and the total cross section curves are depicted in Fig. 3, where Figs. 3(a) and 3(b) are related to the SET I whereas the Figs. 3(c) and 3(d) are related to the SET II. Considering the smaller χ^2/DOF values obtained when $P_{\rm had}$ increases with the energy (FIT III), we believe that this possibility cannot be completely neglected.

In all the cases we see that the data of $\sigma^{\gamma\gamma}_{\rm PYT}$ above $\sqrt{s} \sim 100$ GeV can hardly be described by our model, but this is also a problem for other models in the literature [30] based on the factorization assumption

$$\frac{\sigma_{pp}}{\sigma_{\gamma p}} = \frac{\sigma_{\gamma p}}{\sigma_{\gamma\gamma}}. \tag{19}$$

Assuming the correctness of these models we may interpret the steeper rise of the $\sigma^{\gamma\gamma}$ appointed by the PYTHIA as a possible signal of violation of the factorization relation. Otherwise this behavior indicates a possible failure of the PYTHIA generator at high-energies. The latter possibility is qualitatively supported by the results depicted in the Figs. 3(c) and 3(d), that show that the shape and normalization of the PHOJET cross sections are in good agreement with the factorization relation (19).

V. CONCLUSIONS

Our first aim and main result was to show that an eikonal QCD-inspired model based on a nonperturbative infrared dynamical gluon mass scale [16], with the help of vector meson dominance and the additive quark model, can successfully describe the data of the total photoproduction γp and total hadronic $\gamma\gamma$ cross sections. The calculation is similar to the one of Block *et al.* [9], with the advantage that in the DGM model one has a physical meaning for the infrared scale, and the coupling constant is not a free parameter, turning out to be related to the dynamical gluon mass scale.

We promoted some minor changes in the calculation, assuming that $P_{\rm had}$, the probability that a photon interacts as a hadron, has a logarithmic increase with s. This leads to a improvement in the fit, i.e. it lowers the χ^2/DOF values. There are pros [28] and cons [29] about this possibility. We just point out that the logarithmic increase of $P_{\rm had}$ with s is quite favored by the data.

We verified that the data of $\sigma^{\gamma\gamma}_{\rm PYT}$ above $\sqrt{s} \sim 100$ GeV can hardly be described by our model, but this is also a problem for other models in the literature. Assuming the correctness of these models we could say that the PHOJET generator is more appropriate to obtain the $\sigma^{\gamma\gamma}$ data above $\sqrt{s} \sim 100$ GeV. Connected with this comment we can recall that recently Block and Kaidalov demonstrated that the factorization relation (19) does not depend on the assumption of an additive quark model, but more on the opacity of the eikonal being independent of the nature of the reaction [31]. Hence, according to this result, we argue that it will be difficult for QCD-inspired models incorporating the total cross section factorization hypothesis to accommodate the $\sigma(\gamma\gamma \rightarrow) hadrons$ data with $\sqrt{s}_{\gamma\gamma} > 100$ GeV unfolded with the PYTHIA Monte Carlo generator.

ACKNOWLEDGMENTS

We thank G. Azuelos for the reading of the manuscript. This research was supported by the Conselho Nacional de Desenvolvimento Científico e Tecnológico-CNPq under contracts No. 151360/2004-9 and 301002/2004-5.

[1] H. Cheng and T. T. Wu, Phys. Rev. Lett. **24**, 1456 (1970); G. V. Frolov, V. N. Gribov, and L. N. Lipatov, Phys. Lett. B **31**, 34 (1970).
[2] S. Eidelman *et al.*, Phys. Lett. B **592**, 1 (2004).
[3] M. Derrick *et al.*, Phys. Lett. B **293**, 465 (1992); Z. Phys. C **63**, 391 (1994).
[4] T. Ahmed *et al.*, Phys. Lett. B **299**, 374 (1993); S. Aid *et al.*, Z. Phys. C **69**, 27 (1995).
[5] M. Acciarri *et al.*, Phys. Lett. B **519**, 33 (2001).
[6] G. Abbiendi *et al.*, Eur. Phys. J. C **14**, 199 (2000).
[7] A. Donnachie and P. V. Landshoff, Phys. Lett. B **296**, 227 (1992).
[8] S. Söldner-Rembold, in *Proceedings of the ICHEP 98, Vancouver, 1998* (FREIBURG Report No. FREIBURG-EHEP-98-06, 1998).
[9] M. M. Block, E. M. Gregores, F. Halzen, and G. Pancheri, Phys. Rev. D **60**, 054024 (1999); M. M. Block, F. Halzen, and G. Pancheri, Eur. Phys. J. C **23**, 329 (2002).
[10] G. Pancheri, R. M. Godbole, A. Grau, and Y. N. Srivastava, Acta Phys. Pol. B **36**, 735 (2005); R. M. Godbole, A. Grau, G. Pancheri, and Y. N. Srivastava, Phys. Rev. D **72**, 076001 (2005).
[11] A. Corsetti, R. M. Godbole, and G. Pancheri, Phys. Lett. B **435**, 441 (1998).

[12] K. Honjo *et al.*, Phys. Rev. D **48**, 1048 (1993); L. Durand *et al.*, Phys. Rev. D **47**, R4815 (1993); **48**, 3410(E) (1993).
[13] P. L'Heureux and B. Margolis, Phys. Rev. D **28**, 242 (1983).
[14] B. Margolis *et al.*, Phys. Lett. B **213**, 221 (1988).
[15] L. Durand and H. Pi, Phys. Rev. Lett. **58**, 303 (1987); Phys. Rev. D **38**, 78 (1988); **40**, 1436 (1989).
[16] E. G. S. Luna *et al.*, Phys. Rev. D **72**, 034019 (2005).
[17] A. C. Aguilar, A. A. Natale, and P. S. Rodrigues da Silva, Phys. Rev. Lett. **90**, 152001 (2003).
[18] J. M. Cornwall, Phys. Rev. D **26**, 1453 (1982); J. M. Cornwall and J. Papavassiliou, Phys. Rev. D **40**, 3474 (1989); **44**, 1285 (1991).
[19] J. M. Cornwall and A. Soni, Phys. Lett. B **120**, 431 (1983).
[20] T. Sjöstrand, Comput. Phys. Commun. **82**, 74 (1994); LUND University Report No. LU-TP-95-20, 1995 (unpublished).
[21] R. Engel, Z. Phys. C **66**, 203 (1995); R. Engel and J. Ranft, Phys. Rev. D **54**, 4244 (1996).
[22] G. A. Schuler and T. Sjöstrand, Z. Phys. C **73**, 677 (1997).
[23] A. Capella, U. Sukhatme, C. I. Tan, and J. Tran Thanh Van, Phys. Rep. **236**, 225 (1994).
[24] M. M. Block and K. Kang, Int. J. Mod. Phys. A **20**, 2781 (2005).
[25] V. M. Budnev *et al.*, Phys. Rep. **15**, 181 (1975).
[26] M. Acciarri *et al.*, Phys. Lett. B **408**, 450 (1997).
[27] F. Wäckerle, Nucl. Phys. B, Proc. Suppl. **71**, 381 (1999).
[28] L. Durand and K. Honjo, Report No. MAD/TH/91-12 (unpublished).
[29] J. R. Forshaw, Phys. Lett. B **285**, 354 (1992).
[30] R. M. Godbole, A. Grau, and G. Pancheri, Nucl. Phys. B, Proc. Suppl. **82**, 246 (2000).
[31] M. M. Block and A. B. Kaidalov, Phys. Rev. D **64**, 076002 (2001).